Proceedings of the 4th ACPMG 2024
4th Asia-Pacific Conference on Physical Modelling in Geotechnics
11-13 December 2024, Abu Dhabi, UAE
© 2024 the Authors

Pullout capacity and displacement behavior of opening plate anchor using plane strain box

Mehrzad Shojaee, Mohsen Sabermahani, Emad Mirzaee, Seyed Vahid Mojtahed Sistani

Iran University of Science and Technology, School of Civil Engineering, Tehran, Iran, me_shojaee@alumni.iust.ac.ir, msabermahani@iust.ac.ir

ABSTRACT: In the present paper, the effect of width (B) and embedment ratio (H/B) of a newly designed opening plate anchor on its pullout capacity (P_u) and corresponding displacement (d_u) are investigated experimentally. Two series of 1g small scale physical model tests were implemented in sand with relative density of %75 located in a completely observable box (thin section) that imposed plane strain conditions. In the first series, three pullout tests were performed on opening plate anchors with different width of 120, 150 and 180mm at embedment ratio of 3. It was indicated that anchor width significantly influenced anchor pullout capacity (P_u), but the corresponding relative displacement (d_u/B) stays constant relatively. In second series of tests, three tests were performed on opening plate anchors with different width of 120, 150 and 180mm at embedment ratio of 7. It was concluded that increasing embedment ratio, increases the anchors' pullout load, however it does not change the relative displacement (d_u/B) significantly. Soil deformation field around the anchor was observed using Particle Image Velocimetry (PIV). It was indicated that at embedment ratio of 3, failure surfaces reached the soil surface, but at embedment ratio of 7, plastic zone formed a tunnel shape in the soil and did not cross the soil surface.

1 INTRODUCTION

Many onshore and offshore structures such as wind turbines, chimneys, platforms and pipelines, need uplift resistance supported by anchors (Hanna 1982, Das and Shukla 2013). In order to resist the pullout loads, various types of anchors such as mechanical anchors (plate anchors, pile anchors, drag anchors, helical anchors), grouted anchors and combinations of them are utilized (Kim 2003). Various studies have been performed to investigate the behavior and predict the pullout capacity magnitude of the individual or group of anchors (Ganesh and Sahoo 2016, Ganesh 2019, Roy et al. 2019). It was indicated that plate anchors' pullout capacity can increase to a designed value with increasing the size and depth of anchor or with improving subsoil characteristics such as density or strength (Liu et al. 2012).

One of the common theoretical models states that the pullout capacity of plate anchors, neglecting the anchor's weight, is equal to sum of the weight of soil in the failure zone and resistance force along the failure surface (Mariupol'skii 1965, Das and Shukla 2013). For describing the plate anchors behavior and predicting pullout capacity magnitude precisely, it is vital to obtain a comprehensive understanding of the anchor failure modes. During last decades, various experimental studies have been performed to describe anchor failure modes under different conditions (Balla 1961, Mariupol'skii 1965, Peng et al. 2019).

In spite of numerous researches performed to recognize anchor failure mode, significant differences can be noticed between actual measurements and proposed models. This may be due to a lack of thorough comprehending of interaction between anchors parts and surrounding soil. In order to measure soil deformations around uplifting anchors, many researchers have used image processing techniques (White et al. 2008, Zhang et al. 2018).

In this paper, a brief experimental study of soil deformation field around a plate anchor embedded in sand has been performed, using Particle Image Velocimetry (PIV) method. PIV was implemented to observe the interaction between anchor and surrounding soil and helped to achieve a better understanding of failure surfaces.

The present paper presents two series of small-scaled physical model tests to study the behaviour of opening plate anchor with different widths (B=120, 150 and 180mm), embedment depths (H) and embedment ratios (R=H/B=3 and 7).

2 EXPERIMENTAL SETUP AND MATERIALS

In this study the experimental setup consists of opening plate anchor, plane strain (thin section) box, and data acquisition system (computer, load cell, linear encoder). Data acquisition system was implemented to acquire anchor's pullout load and displacement during the tests. In order to observe soil deformation field around the anchor during pullout tests, PIV photo capturing system captured successive photos of test area in a dark (light adjusted) room.

2.1 Plane strain (thin section) box

A box with dimensions of 1.8 m width, height of 2.2m, 0.1m outer thickness is designed to study opening plate anchor behaviour. Small thickness of the box and also transparent walls leads to proper observations of anchor movements and soil deformation field.
Remarkable thickness of glass walls leads to act as rigid walls with negligible deformations; therefore it is considered that plane strain mode is imposed. As the box is bolted to the ground, it cannot move during the pullout tests. The Detail of plane strain (thin section) box is shown in Figure 1.

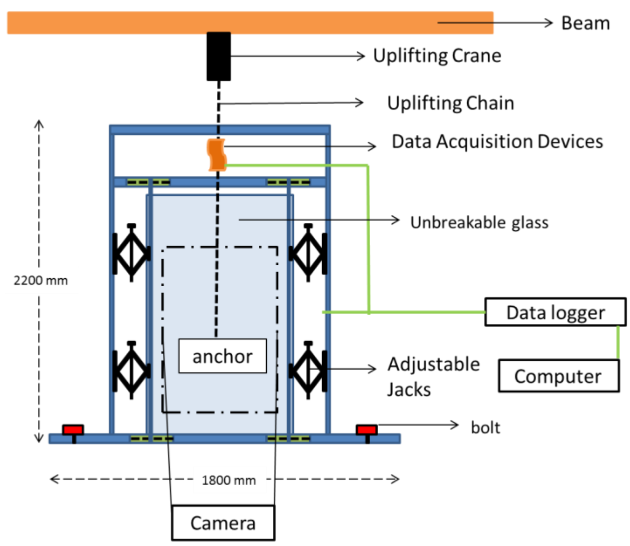

Figure 1. The Detail of plane strain (thin section) box

2.2 Opening plate anchor

"Opening plate anchor" is kind of mechanical anchors with expansive area during pullout. It consists of one or more pair of wings made and a rod made of steel. The steel wings and rod act rigidly during tests. A locked opening plate anchor can be pushed or driven into the soil. After that, the wings are unlocked and opened with help of the spring between the rod and wings. The final opening angle of the wings is equal to 120 degrees and corresponds to the anchor width of equal to B. It this paper, anchor width is equal to 120, 150 and 180mm. The unlocked opening plate anchor detail is depicted in Figure 2.

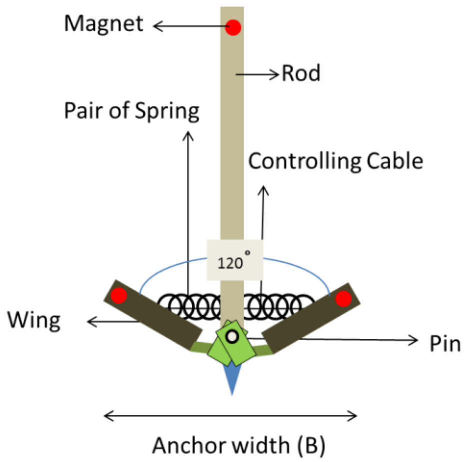

Figure 2. The Detail of unlocked opening plate anchor

2.3 Soil properties

In this research Firoozkooh sand #161 was used. Soil properties are expressed in Table 1. The sample dry unit weight was measured as 15.34 kN/m^3 by dry pluviation method from the height of 1000 mm in accordance with ASTM D698 corresponding to relative density of 75%.
The friction angle is 32° measured in direct shear test in accordance with ASTM D3080 in relative density of 75%.

Table 1. Physical and geotechnical properties of Firoozkooh sand #161

USCS name	SP
Dry unit weight, γ_d ($kN/\mathbf{m}^3$)	15.34
Internal friction angle, Ø	32 °
Relative density, D_R(%)	75%
d_{50}	0.38mm
void ratio (e)	0.68

2.4 Physical model preparation

At first step, the locked opening plate anchor was vertically located at 50 mm depth in the sand bed. Then free magnets (Tracers in PIV system) placement to the glass, corresponding to anchor magnets was done. The upper colored sand layers were located using pulverization and tamping method. A 10 mm-thick colored sand layer was overlaid on each 100 mm sand layer for more accurate and visible observation of sand deformation, until reaching the required height. Finally the connection between measuring instruments (including load cell and encoder) and rod was performed.

3 PIV SYSTEM

Figures PIV (Particle Image Velocimetry) is an image processing method originally developed to observe the global instantaneous displacement of fluids (Adrian 1991). PIV technique is proposed to study soil deformation in geotechnical engineering (White et al., 2003).
It can briefly express that PIV system consists of three parts: tracer particles, image capture system and image processing system (Duan et al. 2018).
In the present research, tracer particles are the soil particles and colored soil lines. Furthermore, free magnets on test box sidewalls were utilized as tracer particles as shown in Figure 3. To capture images, a digital 4K-resolution camera was used. Moreover, the image processing system presented by White et al. (2003) was implemented for PIV analysis.

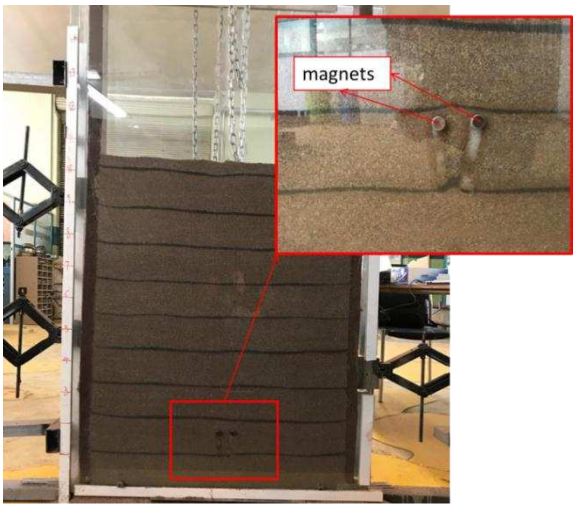

Figure 3. Utilizing magnets as tracer particles in PIV system

4 TESTING SCHEDULE

In this study, two series of tests were implemented to investigate the effects of anchor width (B) and embedment ratio (R=H/B) on anchor pullout capacity (P_u) and its corresponding displacement (d_u).
The tests schedule is shown in Table 2.

Table 2. Use 10 pt both in the headers and the text of Tables.

Series number	R=H/B	B(mm)	Test Name
		120	B12R3
Series 1	3	150	B15R3
		180	B18R3
		120	B12R7
Series 2	7	150	B15R7
		180	B18R7

5 EXPERIMENTAL RESULTS

5.1 Pullout load-upward displacement curves

The pullout load (N)-upward displacement (mm) relationship of the anchor with different anchor widths and embedment ratios are presented in Figure 4.a and Figure 4.b. It should be noted general trend of pullout load-upward displacement curve is similar for all anchors. However there are considerable differences between the behaviors of the shallow and deep anchors. The noted matter is comprehensively discussed in Sabermahani and Shojaee (2021) paper.

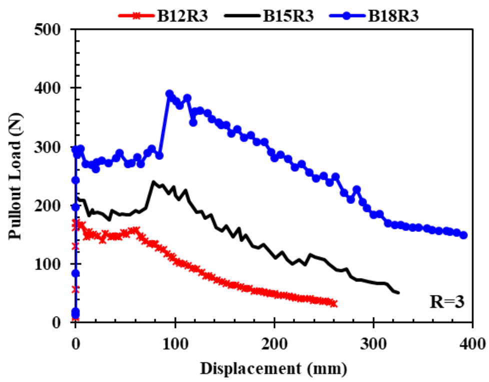

Figure 4.a Pullout load-displacement curves of anchors at embedment ratio of 3.

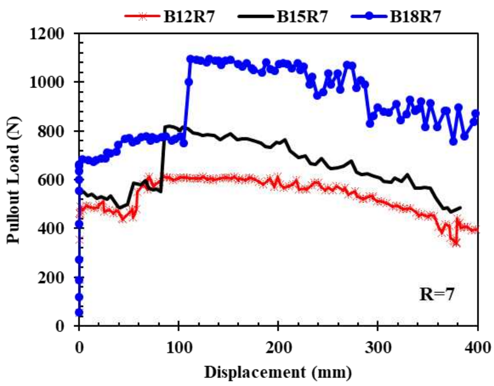

Figure 4.b Pullout load-displacement curves of anchors at embedment ratio of 7.

It can be concluded that for deep anchors (R=7), after reaching the peak pullout load, the pullout value remain constant, but for shallow anchors (R=3), it decreases sharply.

5.2 Pullout capacity and corresponding relative displacement of the anchor

Maximum pullout loads (pullout capacity, P_u) for anchors with different widths at embedment ratio of 3 and 7 are depicted in Figure 5. It is indicated that pullout load increases as anchor width increases. Moreover, increasing embedment ratio leads to a notable increase in anchor pullout capacity.

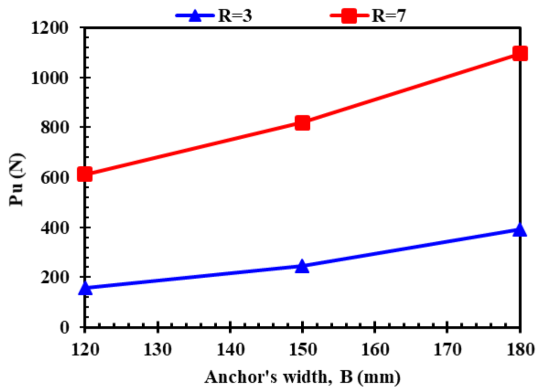

Figure 5. Pullout capacity vs. anchor width at R =3,7

Figure 6 indicates that anchor width or embedment ratio do not affect relative displacement (d_u/B) significantly. For anchors with different widths of 120, 150 and 180 mm with shallow and deep behavior, relative displacement ranged from 0.5 to 0.65.

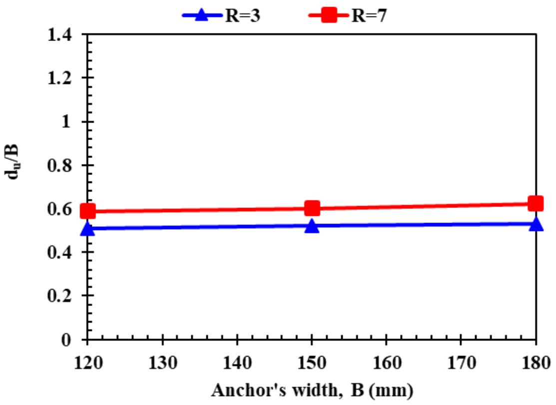

Figure 6. Relative displacement vs. anchor width at R=3,7

6 SOIL DEFORMATION FIELD AND FAILURE SURFACES

To improve the behavior of the opening plate anchor, it is essential to study the soil displacement field around the anchor during the pullout test.
Soil displacement field around the opening plate anchor at instance of maximum pullout load for all presented tests is illustrated in Figure 7.
According to Figure 7, for shallow anchors (R=3) Failure surfaces start from the edge of anchor and reach soil free surface, however for deep anchors (R=7) soil failure surfaces form a tunnel in the soil and do not reach the soil free surface. This stated matter can be an appropriate parameter to distinguish shallow and deep condition for an anchor.

7 CONCLUSIONS

A new-designed expansive plate anchor is studied in this paper. To study the behavior of the anchor, two series of pullout tests in a plane strain (thin section) box were performed and the effects of embedment depth and anchor width on pullout load-displacement curves, pullout capacity (P_u), relative displacement (d_u/B) and soil deformation around the anchor were investigated, using PIV as image processing system. It can be concluded that:

- In present study, the behavior of anchor is recognized as shallow or deep according to (1) pullout load-upward displacement curves and (2) soil deformation field around the anchor using PIV analysis.
- For all shallow and deep anchors (R=3 or 7) as anchor width increases, pullout capacity (P_u) increases significantly, while relative displacement (d_u/B) approximately remains constant.
- For anchors with different width, as embedment ratio (R) increases, pullout capacity (P_u) increases significantly, while relative displacement (d_u/B) ranges from 0.5 to 0.65.
- PIV demonstrated that for shallow anchors, the failure surfaces cross the free soil surface while for deep anchors, failure surfaces do not extend to the free soil surface and shape a tunnel in the soil.

© 2024 the Authors

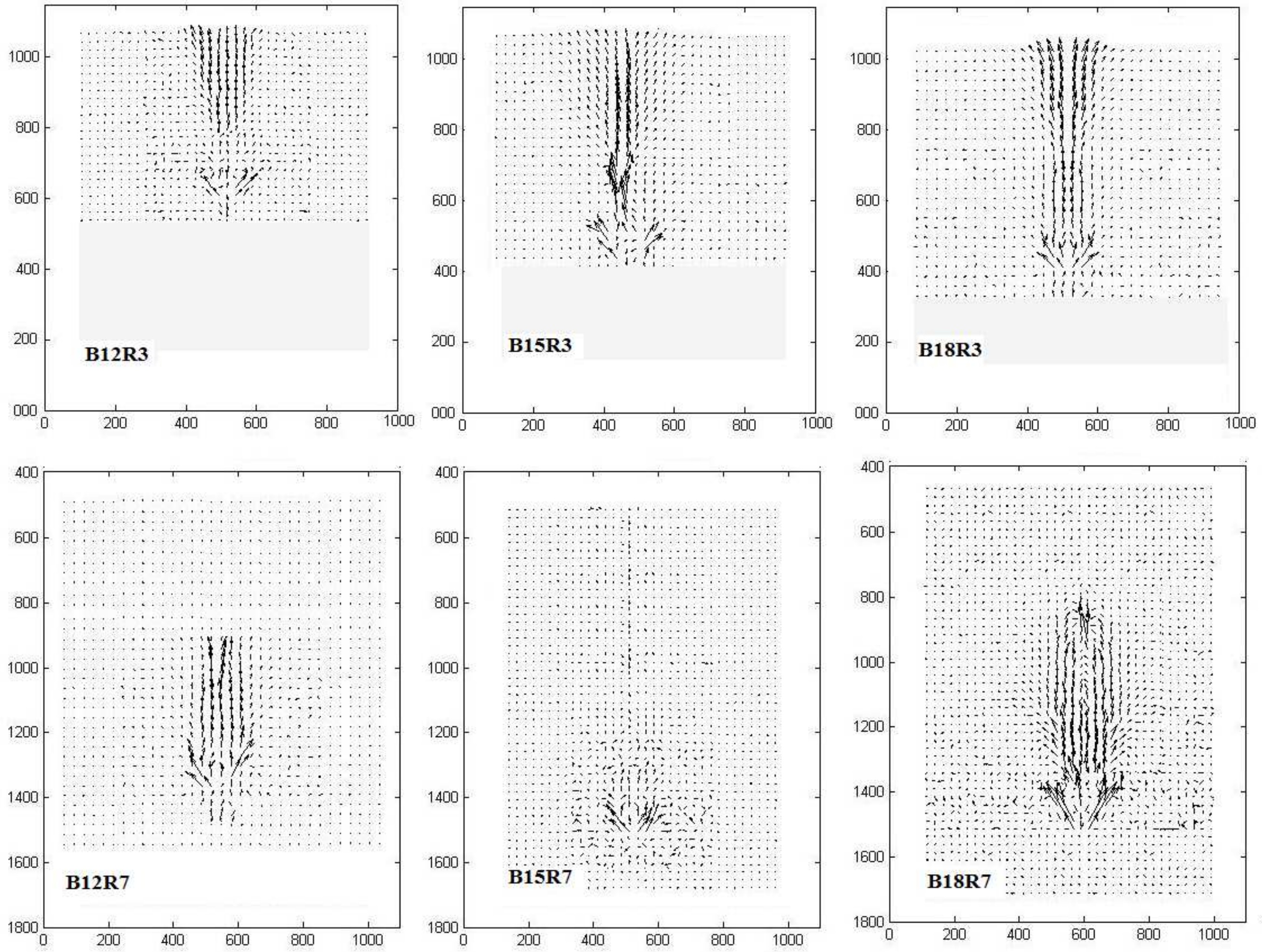

Figure 7. Displacement field at maximum pullout load instance

ACKNOWLEDGEMENTS

This research did not receive any specific grant from funding agencies in the public, commercial, or not-for-profit sectors.

REFERENCES

Adrian, R. J. (1991). "Particle-imaging techniques for experimental fluid mechanics." Annual review of fluid mechanics **23**(1): 261-304.

ASTM D3080- Standard test method for direct shear test of soils under consolidated drained conditions. D3080/D3080M.

ASTM D698-Test Methods for Moisture-Density Relations of Soils and Soil-Aggregate Mixtures." Method A (Standard Proctor).

Balla, A. (1961). "The resistance to breaking-out of mushroom foundations for pylons". Proc. 5 th Int. Conf. on SMFE.

Das, B. M. and S. K. Shukla (2013). "Earth anchors". J. Ross Publishing.

Duan, X.-f., Y.-z. Wang and X.-m. Yuan(2018). "State-of-the-art Review of Particle Image Velocimetry (PIV) in Geotechnical Engineering." DEStech Transactions on Computer Science and Engineering.

Ganesh, R. (2019). "Vertical uplift resistance of close-spaced shallow rectangular group anchor plates embedded in sand." Marine Georesources & Geotechnology: 1-12.

Ganesh, R. and J. P. Sahoo (2016). "Uplift capacity of horizontal strip plate anchors adjacent to slopes considering seismic loadings." Soils and Foundations 56(6): 998-1007.

Hanna, T. H. (1982). Foundations in tension, McGraw-Hill Book.

Kim, N.-K. (2003). "Performance of tension and compression anchors in weathered soil." Journal of

Geotechnical and Geoenvironmental Engineering **129**(12): 1138-1150.
Liu, J., M. Liu and Z. Zhu (2012). "Sand deformation around an uplift plate anchor." Journal of Geotechnical and Geoenvironmental Engineering 138(6): 728-737.
Mariupol'skii, L. (1965). "The bearing capacity of anchor foundations." Soil Mechanics and Foundation Engineering **2**(1): 26-32.
Peng, J., H. Liu, Y. Zhao and K. Liang (2019). "Failure mode and pullout capacity of anchor piles in soils with cohesive and cohesionless properties." Marine Georesources & Geotechnology, 1-14.
Roy, A., Chow, S.H., O'Loughlin, C.D. & Randolph, M.F. (2021). "Towards a simple and reliable method for calculating the uplift capacity of plate anchors in sand." Canadian Geotechnical Journal, 58: 1314–1333.
Sabermahani, M. and M. Shojaee Nasirabadi (2021). "Vertical uplift resistance of an innovative plate anchor embedded in sand." Marine Georesources & Geotechnology: 1-17.
White, D., W. Take and M. Bolton (2003). "Soil deformation measurement using particle image velocimetry (PIV) and photogrammetry." Geotechnique **53**(7): 619-631.
White, D., Cheuk, C., & Bolton, M. (2008). "The uplift resistance of pipes and plate anchors buried in sand." Géotechnique, 58: 771-779.
Zhang, X., J. Liu and M. Liu (2018). "Experimental study on uplift behavior of group anchors in sand." Geotechnical Testing Journal 42(3): 687-702.

INTERNATIONAL SOCIETY FOR SOIL MECHANICS AND GEOTECHNICAL ENGINEERING

This paper was downloaded from the Online Library of the International Society for Soil Mechanics and Geotechnical Engineering (ISSMGE). The library is available here:

https://www.issmge.org/publications/online-library

This is an open-access database that archives thousands of papers published under the Auspices of the ISSMGE and maintained by the Innovation and Development Committee of ISSMGE.

The paper was published in the proceedings of the 4th Asia-Pacific Conference on Physical Modelling in Geotechnics and was edited by Tarek Abdoun. The conference was held from December 11th to December 13th 2024 in Abu-Dhabi, United Arab Emirates.